RSC Advances

Tribological Behavior of WS_2-based Solid/Liquid Lubricating Systems Dominated by Surface Property of WS_2 Crystallographic Planes

Xin Quan[1, 2], Xiaoming Gao[1], Lijun Weng[1], Ming Hu[1], Dong Jiang[1], Desheng Wang[1], Jiayi Sun[1, *], Weimin Liu[1,*]

[1] State Key Laboratory of Solid Lubrication, Lanzhou Institute of Chemical Physics, Chinese Academy of Sciences, Lanzhou 730000, PR China

[2] University of Chinese Academy of Sciences, Beijing 100049, PR China

Abstract

In this paper, the WS_2-based solid/liquid systems were established successfully by combining pure WS_2 film with FCPSO (trifluorinated-propyl and chlorinated-phenyl with methyl terminated silicone oil) and SiCH (silahydrocarbons) space oils, and the tribological performances and mechanisms were investigated. The results showed that the tribological properties of the WS_2 film were improved greatly as associated with the SiCH oil, and hence this composite system exhibited a low/stable friction coefficient (<0.08) and durable wear life (>3×10^6 sliding cycles) both in vacuum and air environments. However, a reverse effect was obtained from the WS_2 film/FCPSO system. The selective adsorption of WS_2 crystallographic planes with the specific oil seemed to dominate the tribological performances of the composite systems. The SiCH and FCPSO oils have different affinity with the base and edge planes, respectively, as composited with the WS_2 film. The combination of WS_2 base plane with SiCH was more advantageous to form perfect lubricating and transfer films at the friction contact area, resulting in the improved friction and wear performances. This result pay a significant way for us to design the solid/liquid lubricating system based on the lamellar solid lubricants.

1.Introduction

Up to now, solid and liquid lubrication, as the traditional and principal technologies, are used to deal with tribological problems in the space mechanisms, whereas, each

* Corresponding author. E-mail: sunjy@lzb.ac.cn (J. Sun).Tel.: +86 931 4968092; fax.:+86 931 8277088.
* Corresponding author. E-mail: wmliu@licp.cas.cn (W. Liu).Tel.: +86 931 4968166; fax.:+86 931 8277088.

has specific disadvantages.[1, 2] Novel lubrication systems with lower friction and wear are needed to meet the new frontier of space mechanisms [3-5]. It has been proved that combining liquid and solid lubricants on sliding tribological surfaces may be effective to reduce friction and wear, especially under the boundary lubricating condition.[6-14] In this field of research, the solid lubricants are mainly focused on hard materials (such as DLC, Si_3N_4, ZrO_2, etc.), as the high hardness is beneficial for improving the load capacity of composite systems.[9, 13, 15]

Sputtered films of transition metal disulfides, typical for MoS_2 and WS_2, have been widely used in the space technology due to the low friction coefficient in vacuum,[15-21] but the wear life is limited because of the porous columnar microstructure. The sputtered WS_2 film was characterized by a duplex-layer microstructure. The dense lower layer exhibits a basal plane orientation, while the porous upper layer predominantly has an edge plane orientation.[17, 18, 22] Due to the anisotropy of WS_2 crystal in the mechanical property, the base-plane oriented layer has a better load capacity, while the edge-plane oriented layer fractured easily in the process of sliding friction.[23-25] It was suggested that the tribological properties of the sputtered WS_2 film should be improved by compositing with liquid lubricants.

However, it is very notable for lamellar crystal solids like WS_2, MoS_2 and graphite. The basal and edge planes have different surface properties.[26, 27] The basal plane has a relatively low polarity and surface energy. On the contrary, the edge plane is polar and volatile for the existence of dangling and unsaturated bonds, along with a much higher surface energy.[24] Previous studies revealed that as MoS_2 and graphite were mixed with different solvents,[28, 29] the difference in the surface property between the crystallographic planes can result in an interesting selective adsorption phenomenon to minimize the potential energy of these systems. Comparatively, the non-polar basal plane areas preferentially adsorbed weak polarity hydrocarbon chains especially for long methylene chains, while the polar edge sites independently adsorbed polar compounds.[26, 27, 29-34] Therefore, it is reasonable to speculate that the distribution, wettability and the bond conditions of the oils at the WS_2 film surface should be different as they were composited. That may lead to the different friction and wear behavior. In the present work, two specific liquid lubricants with distinct polarity and structure, FCPSO (trifluorinated-butyl and chlorinated-phenyl with methyl terminated silicone oil) and SiCH (silahydrocarbons), both of which have been successfully used in space mechanisms and they were selected to composite with the sputtered WS_2 films, and the friction and wear behavior of both composite systems were deeply investigated.

2. Experimental detail

2.1. Preparation of WS_2-based solid/liquid lubrication system

The two solid/liquid lubrication systems were fabricated by compositing the RF-sputtered WS_2 films with the FCPSO and SiCH oils respectively.

Firstly, the pure WS_2 films were deposited on AISI 440C steel and commercial n-type Si (100) substrates using a WS_2 target (80 mm in diameter, 99.9% purity) by a RF sputtering system, which were respectively used for the tribological and structural analyses. Before the deposition, the AISI 440C (Ø25 mm × 4 mm) substrates were polished to a surface roughness (*Ra*) ≤ 0.03μm and then cleaned with alcohol and acetone ultrasonically for 10 min in sequence. when the chamber vacuum was evacuated to a base pressure below 1.0×10^{-3} Pa, the substrate surfaces were etched by an Ar plasma for 10 min at a DC bias of -500 V to eliminate possible contaminants. Afterwards, the WS_2 films were sputtered under a target power density of 0.062 $W\cdot mm^{-2}$, a substrate bias voltage of -30 V and an Ar pressure of 3.0 Pa. The deposition duration was 15 min. During the deposition, the substrate was statically placed opposite to the target, and the vertical distance between the target and substrate surfaces was 60 mm.

Secondly, the SiCH and FCPSO were coated on the pre-deposited film surfaces by a spin coating method, respectively. The WS_2-based solid/liquid lubrication system was composed of an upper oil layer with a thickness about 20 μm and an under WS_2 layer with a thickness about 3 μm. The thickness of oil film was evaluated as following: Firstly, the mass ($\boldsymbol{m_1}$) of the disk was measured by analytical balance with accuracy of one over ten-thousand, then we used a manual microinjector to add several drops of oil to the middle of the WS_2 film surface. Secondly, the oil was spread by spinning the disk for 30 min with a rotational speed of 1000 rev/min. In this process, a part of oil would be thrown away from the disk for centrifugation. After the spinning, the excess oil on the edge of disk was removed by wiping with a silk cloth. And then, the mass ($\boldsymbol{m_2}$) was weighed again. Therefore, the pure mass of the oil spread on the surface of WS_2 film was $\boldsymbol{m}$ ($\boldsymbol{m=m_2-m_1}$). And the volume of the oil was calculated by the formula: $\boldsymbol{v=m/\rho}$ (where $\boldsymbol{v}$ is the volume, $\boldsymbol{m}$ the mass, and $\boldsymbol{\rho}$ the density of oil). It was approximately thought that the oil film was evenly spread out in the film surface, then the thickness of oil film could be evaluated: $\boldsymbol{h=v/s}$ (where $\boldsymbol{h}$ is the thickness, $\boldsymbol{v}$ the volume, and $\boldsymbol{s}$ is the bottom area of disk).

Then, the WS_2-based solid/liquid composited lubrication systems were successfully formed for follow-up tests. The SiCH and FCPSO oils were synthesized by the State Key Laboratory of Solid Lubrication, Lanzhou Institute of Chemical Physics, suitable for space applications due to the extremely low volatility, high viscosity index, wide running temperature, low pour point and excellent lubrication property,[35-37] and their typical properties are listed in Table 1.

Table 1 Typical properties of SiCH and FCPSO oils

	SiCH	FCPSO
Average molecular weight	872	9000
Molecular structure	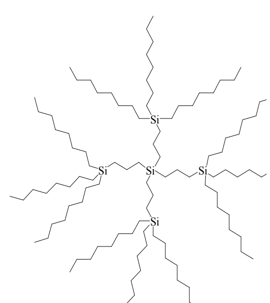	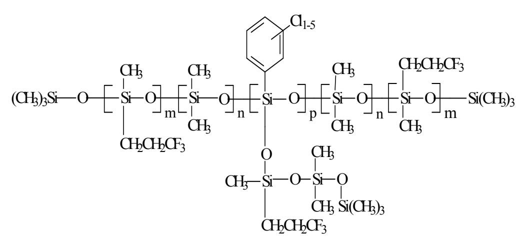
Viscosity at 40°C/$mm^2 \cdot s^{-1}$	97	109
Viscosity at 100°C/$mm^2 \cdot s^{-1}$	17.0	34.0
Viscosity index	194	350

Density at 20°C/kg·m^{-3}	842.5	1113.0
Vapor pressure at 20°C/Pa	2.7×10^{-7}	3.1×10^{-9}

2.2. Friction and wear tests

The friction and wear tests for the composited systems were carried out by a ball-on-disk tribometer in vacuum (lower than 5.0×10^{-3} Pa) and atmospheric environment (30% RH, 20±5 °C). The tribological properties of the pure WS_2 film and oils were also tested for comparison. The upper specimens were the cleaned AISI 440C steel balls (HRC~60, Ra~0.10 μm) of 8 mm in diameter, loaded against rotating discs with a normal load of 3 N. The rotational speed was 1000 rev/min for all tests, corresponding to a linear speed of 0.52 m/s. Each friction test was repeated three times under the same conditions. After the friction tests, the wear track profiles were analyzed by a non-contact 3D surface profiler (AD Corporation, Massachusetts, USA), and then the wear rates ($\boldsymbol{W}$) were calculated by the formula:

$$\boldsymbol{W} = \frac{\boldsymbol{V}}{\boldsymbol{F}\cdot\boldsymbol{L}}$$

where $\boldsymbol{V}$ is the wear volume, $\boldsymbol{F}$ the normal load, and $\boldsymbol{L}$ the total friction distance.

The theoretical minimum film thickness ($\boldsymbol{h_{min}}$) and its ratio with roughness ($\boldsymbol{\lambda}$) were calculated using Eq. (1) and Eq. (2). The calculated λ parameter was 0.263 for WS_2/SiCH and 0.403 for WS_2/FCPSO which state that the lubrication regime for the two lubrication systems were boundary lubrication ($\boldsymbol{\lambda}$ <1). The surface roughness of WS_2 film deposited on disk *Ra* was about 0.5 μm measured by 3D surface profiler. The load of 3 N resulted in an initial average Hertzian contact stress ($\boldsymbol{P_0}$) about 0.25 GPa and theoretical contact radius ($\boldsymbol{a}$) about 0.75×10^{-4} m calculated by Eq. (3) and Eq. (4).

$$\frac{h_{min}}{R'} = 3.63\left(\frac{U\eta_0}{E^*R'}\right)^{0.68}(\alpha E^*)^{0.49}\left(\frac{w}{E^*R'^2}\right)^{-0.073}\left(1-e^{-0.68k}\right)\ldots(1)$$

$$\lambda = \frac{h_{min}}{\sqrt{\sigma_1{}^2+\sigma_2{}^2}}\ldots(2)$$

$$P_0 = \left(\frac{6WE^{*2}}{\pi^3R'^2}\right)^{1/3}\ldots(3)$$

$$a = \left(\frac{3WR'}{4E^*}\right)^{1/3} \ldots(4)$$

where R' is the reduced radius of curvature, U is the entraining surface velocity, W is the normal load, E^* is the reduced Young's modulus, η_o is the dynamic viscosity, α is the pressure–viscosity coefficient, σ_1 is the surface roughness of ball and σ_2 is the surface roughness of lower disk.

2.3. Characterization

The morphology of WS_2 film was observed by a JSM-6701F field emission scanning electron microscopy (FESEM). After the friction tests, the structure of oils was analyzed by the IFS 66v/s Fourier transformation infrared spectroscopy (FTIR). The morphology and composition of the worn surfaces were examined by the JMS-5600L JEOL scanning electron microscopy (SEM), energy dispersive spectrometry (EDS) and X-ray photoelectron spectroscopy (XPS). Before the characterization, the steel balls were ultrasonically cleaned for 5 minutes in proper solvents. The wear debris for the composited systems after the vacuum friction tests were collected and rinsed, and then examined by the JEM-1200EX/S transmission electron microcopy (TEM).

3. Results and discussion

3.1. Structure of sputtered pure WS_2 film

The structure of studied WS_2 film has been investigated systematically and reported in elsewhere.[17, 18, 25] It can be characterized by a duplex layer structure, common for the sputtered MoS_2 film,[22, 38] and the typical surface and cross-sectional FESEM micrographs were shown in Fig. 1. The lower was a dense and coherent layer (about 100 nm) near the interface of film and substrate, where the crystallites were normally characterized by a basal plane oriented growth. The upper was a loose columnar platelet layer with a predominantly edge plane oriented growth. This structure was a zone 2 morphology based on the Thornton's structure zone model.[39]

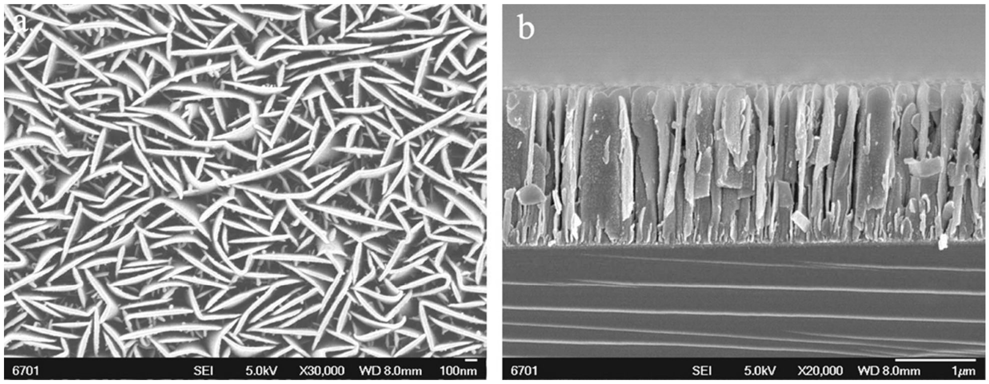

Fig. 1 FESEM micrographs of RF-sputtered WS_2 film: a. surface and b. cross-section

3.2. Friction and wear performances

Fig. 2a shows the typical friction curves of the pure WS_2 films under air and vacuum conditions. The wear life was defined as the sliding cycles before the friction coefficient exceeding the value of 0.25. Clearly, for the WS_2 film the tribological properties were better in vacuum than in air. In vacuum, the friction coefficient was low and stable, and the wear life was much longer. The mean friction coefficient and wear life were 0.09 and ~4.1×10^5 r in vacuum, and 0.12 and ~0.56×10^5 r in air. The deterioration of the tribological properties mainly resulted from the oxidation process of O_2 or H_2O in ambient for the existence of unsaturated or dangling bonds at the WS_2 edge planes.[22] The lubricating properties of both FCPSO and SiCH oils for the steel/steel test pair were investigated comparatively and the typical friction curves of 1.2×10^5 cycles were shown in Fig. 2b. The mean friction coefficients in vacuum and air conditions were ~0.13 and 0.15 for FCPSO, and both ~0.10 for SiCH, respectively.

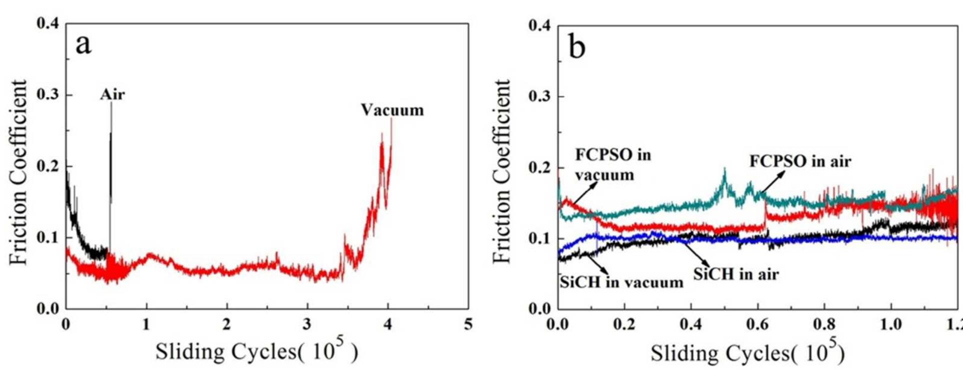

Fig. 2 Friction curves: a. pure WS_2 film in vacuum and air, b. liquid lubricants under steel/steel contacts in vacuum and air

Fig. 3 shows the typical friction curves of the WS_2/FCPSO and WS_2/SiCH lubrication systems in vacuum and air. For the WS_2/FCPSO lubrication system (see in Fig. 3a), both in air and vacuum, the friction coefficients were relatively stable only in the beginning stage, and then became fluctuant and high until the lubrication failures after the sliding cycles of 0.46×10^5 and 0.57×10^5 in air and vacuum, respectively. For the WS_2/SiCH lubrication system (see in Fig. 3b), the friction coefficient was as low as 0.06 and kept stable either in vacuum or air even as the sliding had been lasted up to 30×105 cycles, which was obviously superior to the former.

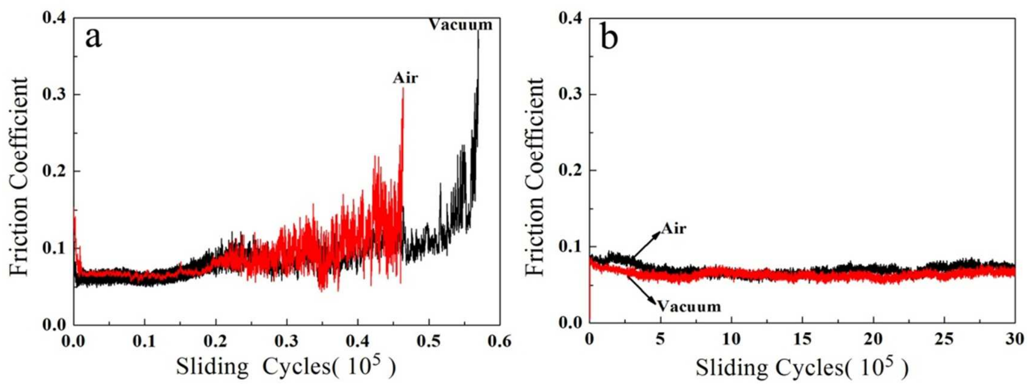

Fig. 3 Friction curves of solid/liquid lubrication systems in vacuum and air: a. WS_2/FCPSO; b. WS_2/SiCH

The wear rates of the WS_2 film, WS_2/FCPSO and WS_2/SiCH lubrication systems were shown in Fig. 4. In comparison, the WS_2/SiCH lubrication system exhibited a very well wear resistance both in vacuum (the wear rate was about 3.0×10^{-8} mm^3/Nm) and air (about 4.2×10^{-8} mm^3/Nm). However, WS_2/FCPSO lubrication system exhibited a poor wear resistance both in vacuum (the wear rate was about 1286.6×10^{-8} mm^3/Nm) and air (about 1009.3×10^{-8} mm^3/Nm). The wear rates in both vacuum and air increased in the following order: WS_2/SiCH < WS_2 < WS_2/FCPSO. In summary, to combine the WS_2 film with only suitable oil can generate a synergistic lubrication effect and result in the improved tribological property. Therefore, it was noticed that the selection of oils should be careful, because the opposite action could be obtained from the different composite systems, such as WS_2/SiCH and WS_2/FCPSO. For different lubrication conditions, the friction and wear results were summarized in Table 2 and Fig. 4.

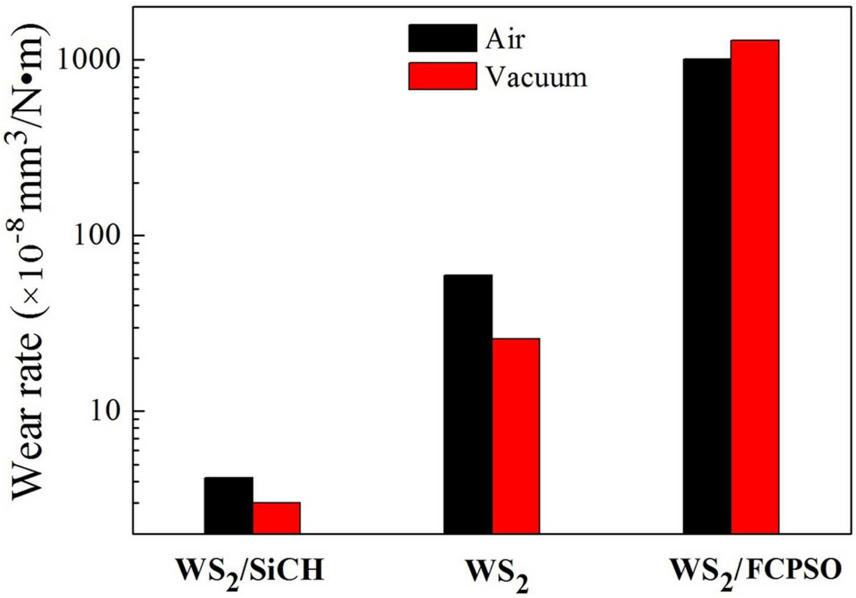

Fig. 4 Wear rates of the solid/liquid lubrication systems and pure WS_2 film

Table 2. Mean friction coefficient of the oils, WS_2 film and their composite systems in vacuum and air environments

	FCPSO (Steel/Steel)	SiCH (Steel/Steel)	WS_2	WS_2/FCPSO	WS_2/SiCH
Vacuum	0.13	0.10	0.09	0.09	0.06
Air	0.15	0.10	0.12	0.09	0.07

3.3. Friction and wear mechanism

Fig. 5 gives the analysis results of the FTIR spectra of SiCH and FCPSO before and after friction tests. The oils for FTIR analysis after the friction tests were collected from the wear track surfaces of composite systems. There were no obvious structure changes for FCPSO after the friction tests in both vacuum and air as well for SiCH in air. Only for SiCH in vacuum, it was found that a new characteristic peak of C=O at 1726 cm^{-1} appeared after the tribotest, suggesting that an oxidative polymerization process might be generated under this condition.[40] The more specific scanning of this new peak from 1780 cm^{-1} to 1680 cm^{-1} was showed as an inlet in Fig. 5c. However, the carbonyl was not detected even after the sliding of 20×10^5 cycles in vacuum for SiCH. Therefore, it can be concluded that this structure change of SiCH in vacuum was not mainly responsible for the vacuum friction and wear behavior of the WS_2/ SiCH system. No oxidative polymerization detected for SiCH after test in air condition seems to be the reason that the nascent steel surfaces were absent under high oxygen atmosphere, which could afford a key catalysis action for this process.[40]

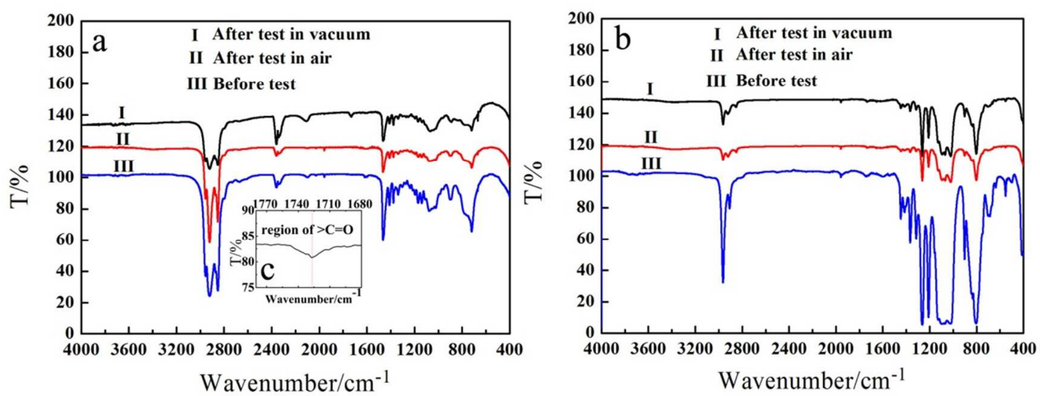

Fig. 5 The FIRT spectra of liquid lubricants before and after the tribotests: a. SiCH, b. FCPSO, c. specific scanning of SiCH after test in vacuum

During the friction process, the FCPSO oil might produce many Si-containing or O-containing species with the strong polarity under the repeated shearing of the loaded pressure, which should have preferential affinity with the edge sites of the WS_2 film. However, there are many long hydrocarbon chains in the structure of SiCH molecules, such as octyl or decyl groups, which would be preferentially adsorbed with the basal plane of WS_2 film. In the beginning of friction process, the upper WS_2 columnar platelets were cracked under the shearing action,[16] and then a plenty of WS_2 fragmentation would be mixed with the liquid lubricant to form an upper lubrication layer. In this stage, the mixed layer seems to mainly afford the effective lubrication. That's why the relatively low and stable friction coefficients were shown up in the initial stage for the two systems. The duplex lubricating layers, composed of the upper mixed layer and lower thin WS_2 denser layer, were firstly established.

As the sliding continued, the selective adsorption could occur when the oil sufficiently contacted with the WS_2 fragmentation. Obviously, the oil layer would firstly occupy the surface of the counterpart ball due to its low surface energy. Thus, the transferring action of WS_2 film to counterpart ball may be sensitive to the selective adsorption. In order to confirm this surmise, the friction tests with different sliding cycles were implemented, and then the morphology and chemical composition of the wear tracks and wear scars on the counterpart ball were analyzed in detail. Figs. 6 and 7 as well as Table. 3 and 4 show the SEM images and EDS results of the wear scars on the steel balls for the WS_2/FCPSO and WS_2/SiCH systems after different vacuum sliding cycles, respectively. For WS_2/FCPSO system (Fig. 6 and Table. 3), no obvious wear scar were observed by SEM and element weight percent (wt %) of W and S were detected from the steel ball surface after 0.1×10^5 cycles, indicating that the oil may play an important role in the relative low and stable friction in the beginning sliding stage. Afterwards, the W and S elements were detectable from the friction contact areas on the steel ball surfaces and the contents increased with the sliding cycles, but still limited (the highest sum of W and S contents $\leq$ 4 at.%). Therefore, the effective transfer film of WS_2 was not observed even after the lubrication failed, expect for some scratches were observed from the wear scars. However, for the WS_2/ SiCH system, the morphology and composition of the wear scars was quite distinct from that of WS_2/ FCPSO. The wear scar was smooth and the signal of W and S elements were not detected by EDS analysis until the sliding cycles higher than 0.5×10^5 cycles, indicating that the sliding cycles of SiCH were longer than that of FCPSO when the lubrication was mainly provided by the oil composited with the WS_2 films. Afterwards, the transfer film was observed clearly and became more and more continuous and dense as the sliding cycles increased (Fig. 7b, 7c and 7d), accompanied by a relatively high and gradually increased contents of W and S elements. These results indicated that the composited oils had an important influence on the transferring of WS_2 film to the counterpart surface. In comparison, to composite with the SiCH oil was conducive to the formation of a continuous and dense transfer film on the counterpart surface. Correspondingly, better tribological performances were obtained from the WS_2 film-SiCH composite system.

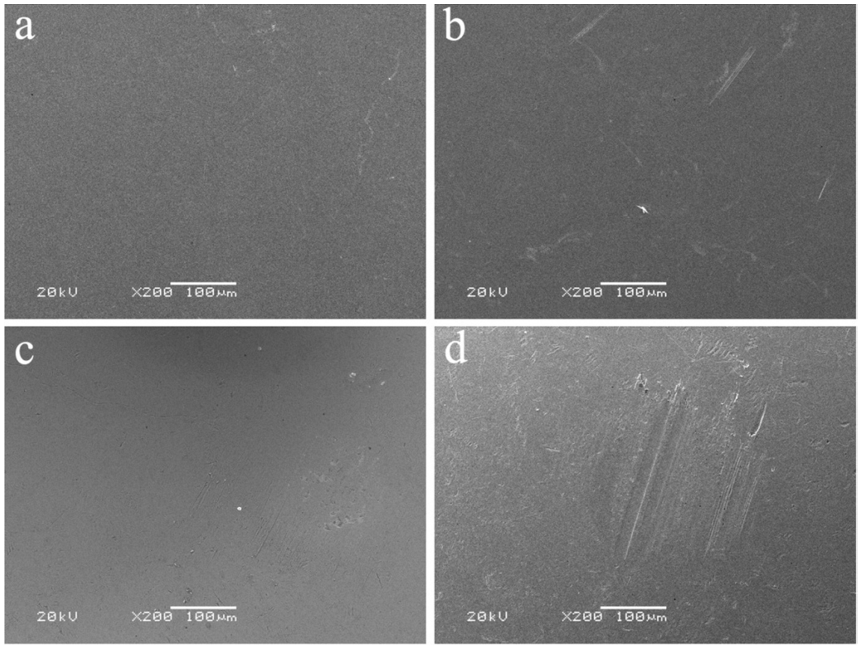

Fig. 6 Typical SEM micrographs of the steel ball in vacuum for WS_2/FCPSO system after different sliding cycles: a, for 0.1×10^5 cycles; b for 0.2×10^5 cycles; c for 0.3×10^5 cycles; d for 0.57×10^5 cycles

Table 3. Comparisons of the element weight percent (wt %) of the wear scar from EDS analysis for WS_2/FCPSO system in vacuum after different sliding cycles

cycles （$\times10^5$）	S (wt %)	W (wt %)	Fe (wt %)	Cr (wt %)
0.10	0.00	0.00	98.33	1.67
0.20	0.00	1.04	97.28	1.68
0.300	0.32	2.98	76.81	19.89
0.57	0.24	3.67	94.41	3.68

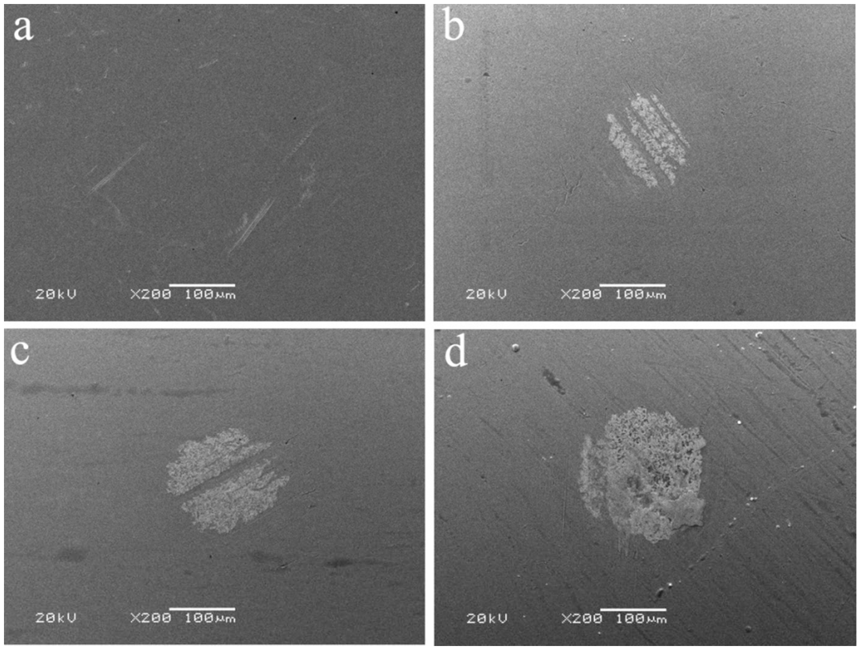

Fig. 7 Typical SEM micrographs of the steel ball in vacuum for WS_2/ SiCH system after different sliding cycles: a for 0.5×10^5 cycles; b for 5×10^5 cycles; c for 15×10^5 cycles; d for 30×10^5 cycles

Table 4. Comparisons of the element weight percent (wt %) from EDS analysis of the wear scar for WS_2/SiCH system in vacuum after different sliding cycles

cycles ($\times10^5$)	S (wt %)	W (wt %)	Fe (wt %)	Cr (wt %)
0.5	0.00	0.00	97.98	2.02
5.0	0.85	13.66	83.78	1.71
15.0	0.74	35.34	49.84	14.07
30.0	1.49	66.68	28.40	3.43

To further elucidate the friction and wear mechanism, the SEM and 3D images of the wear tracks after the friction tests were investigated in detail as shown in Figs. 8 and 9. It could be seen that a great deal of bulky fragmentation wear debris accumulated along the edges and inside of wear track for pure WS_2 film (Fig. 8a-b and Fig. 9a-b), suggesting that the films underwent the adhesive wear as well as severe plastic deformation.[18] The bulky fragmentation wear debris, generated from the section of collapsed columns or fibers after sliding, was due to the porous microstructure.[22] Fig. 8e and 8f show that wear tracks for WS_2/SiCH system were relatively smooth and narrow. The calculated theoretical Hertzian diameter was about

150 µm. In Fig .8, the wear track widths of WS_2/SiCH system (220 µm in vacuum and 210 µm in air) were closer to the theoretical Hertzian diameter than those of WS_2/FCPSO system (350 µm in vacuum and 310 µm in air). In comparison, it can be seen the wear tracks for the WS_2/FCPSO system were wide and deep from Fig. 8c and 8d. Moreover, a ribbon-like pitting wear trace was observed in the middle of wear tracks both in vacuum and air conditions in Fig. 8g and 8h, indicating that the films in these regions were peeled off. The XPS analysis result of the wear track surface in vacuum for WS_2/FCPSO could further support the lower denser film was scratched, thus leading to the exposing of steel substrate. F1s peak at the binding energy of 685.2 eV (Fig. 10) was in agreement with metal fluoride,[41] generating from the tribochemical reaction by FCPSO and the substrate surface metal atoms during the sliding process. Finally, the pitting phenomenon appeared, corresponding to the shorter wear life and higher friction coefficient for WS_2/FCPSO lubrication system.

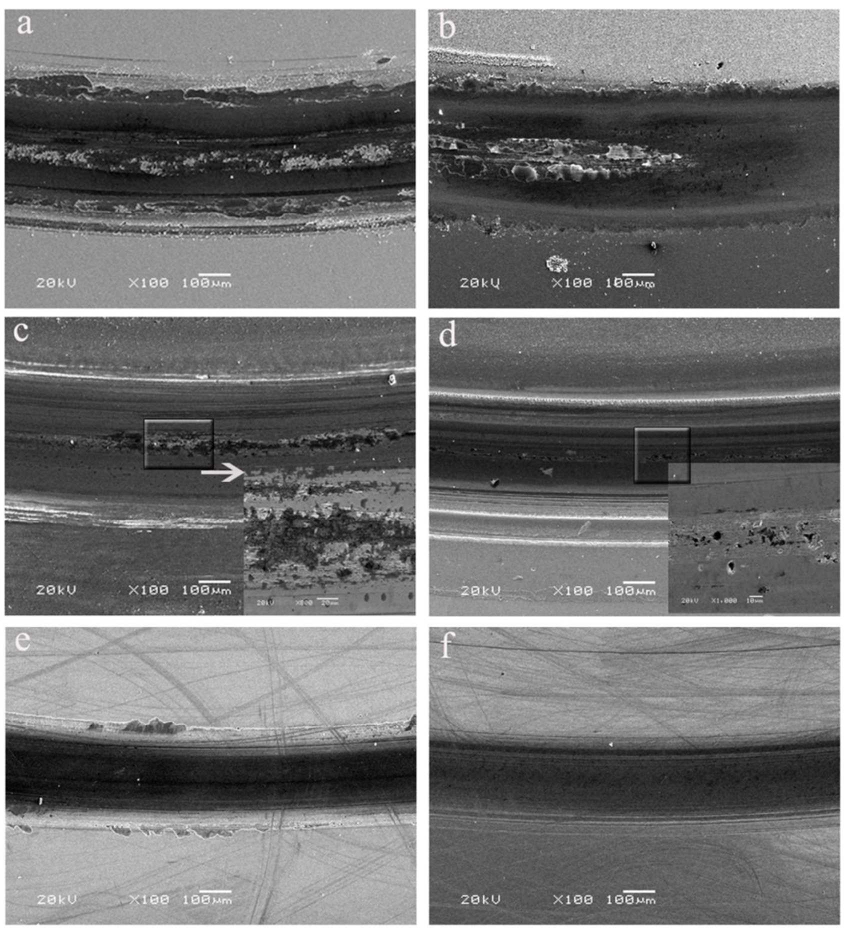

Fig. 8 SEM micrographs of the worn surfaces: a. WS_2, c. WS_2/FCPSO, and e.

WS$_2$/SiCH in vacuum; b. WS$_2$, d. WS$_2$/FCPSO, and f. WS$_2$/SiCH in air; g. magnification of the marked area in c, h. magnification of the marked area in d

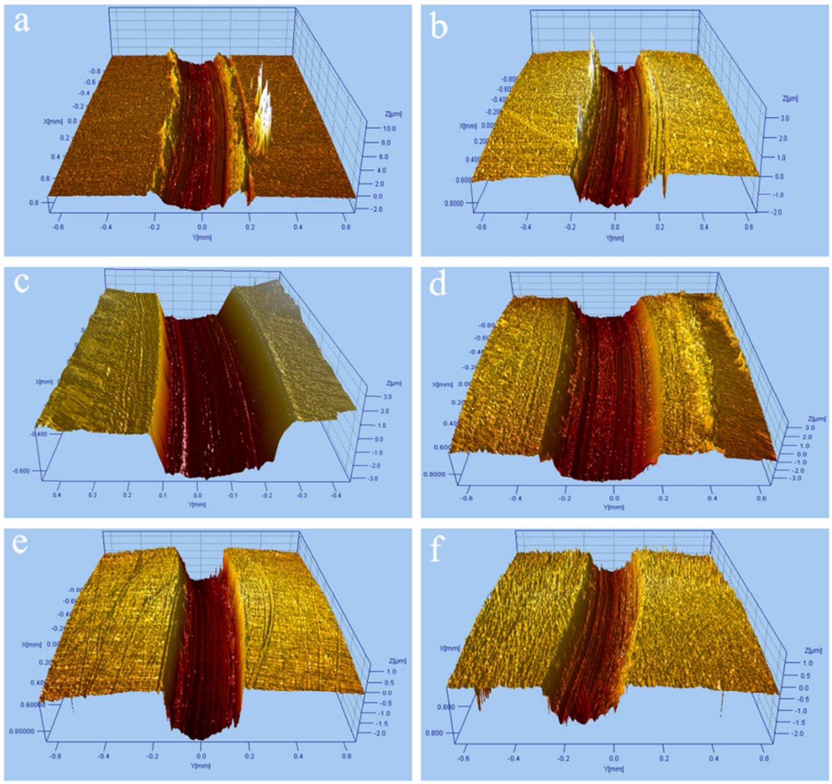

Fig. 9 3D non-contact surface profiler images of the wear tracks: a. WS$_2$, c. WS$_2$/FCPSO, e. WS$_2$/SiCH in vacuum; b. WS$_2$, d. WS$_2$/FCPSO, f. WS$_2$/SiCH in air

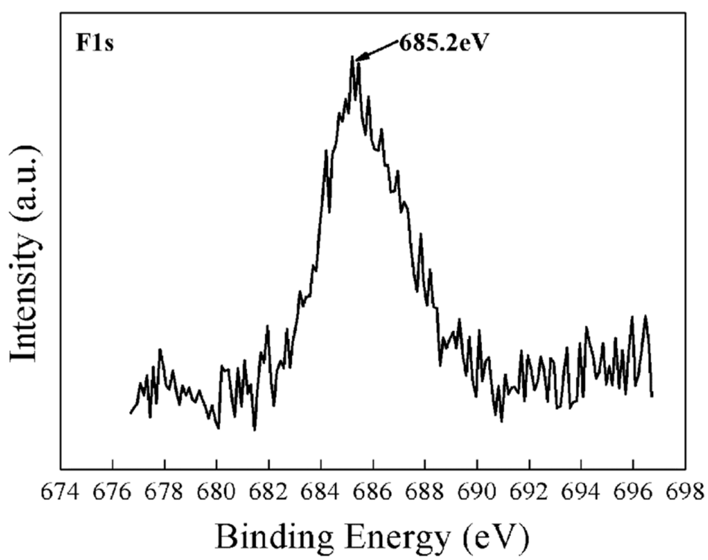

Fig. 10 XPS F 1s spectrum from the wear track surface of WS$_2$/FCPSO system in vacuum

Based on the results discussed above, the friction and wear mechanism of the WS_2-based composite systems could be proposed. Apparently, the selective adsorption of WS_2 crystallographic planes on FCPSO and SiCH was the focus which governs the friction and wear mechanism. The results of TEM morphology images of wear debris can give the explanation on the mechanism from another perspective. It is clear from the Fig. 11a that the plate-like WS_2 thin nanosheets were observed after 30×10^5 cycles friction testing in vacuum for WS_2/SiCH system. In comparison, a plenty of clavate-like debris with low aspect ratio was founded for WS_2/FCPSO system after friction testing from Fig. 11b. This result was in well agreement with the previous studies that basal plane crystals of graphite as well MoS_2 always present a relatively higher aspect ratio than edge site crystals.[28, 29, 42] Additionally, the basal planes adsorbed with oil would have easy access to the rubbing metal surface and interact with it by the basal plane sulphur atmos, decreasing the metal surface energy and increasing the load carrying capacity of steel.[27] Therefore, the plate-like WS_2 debris should have higher proportion possessing the basal orientation. Plate-like WS_2 debris were very likely to lie flat with the worn metal surfaces to effectively prevent the metal to metal direct contacting and even repair them, generating a favorable tendency to form complete lubricating film on the rubbing surface for WS_2/SiCH system. Whereas, for WS_2/FCPSO system, the relatively hard edge plane WS_2 debris adsorbed with FCPSO were more likely to embed in the lower film and even the rubbing metal surfaces to scratch them.[23, 27] Thus, the chances of direct contacting of metal to metal increased highly, resulting in the abrasion became more pronounced. Of course, the formation of transfer films for composite systems were also strongly affected by the special adsorption. Because the complete lubricating film on the rubbing surface and high aspect ratio WS_2 films was more beneficial to transfer on counterface. The schematic diagram of the possible friction and wear mechanisms were showed in Fig. 12.

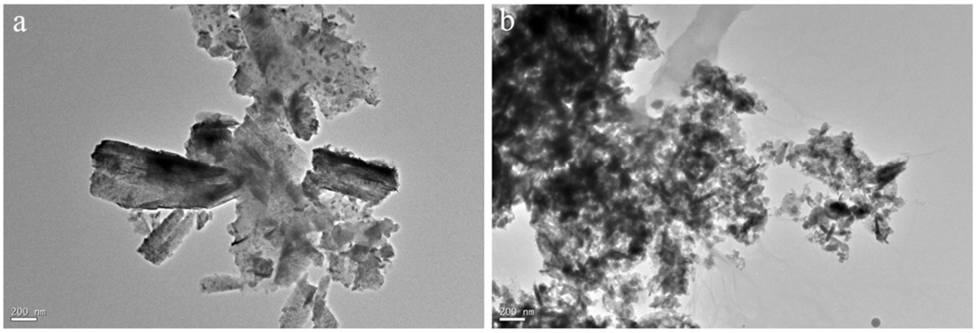

Fig. 11 Typical TEM pictures of worn debris after the vacuum friction test: a, WS_2/SiCH system; b, WS_2/FCPSO system

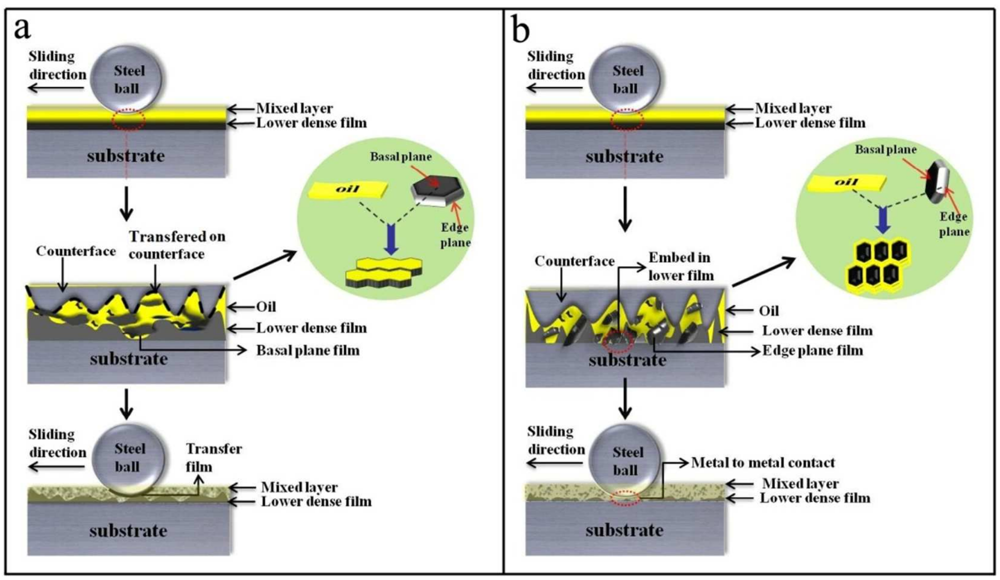

Fig. 12 Schematic diagram for explaining the possible friction and wear mechanisms: a, WS_2/SiCH system; b, WS_2/FCPSO system

Thus, the solid/liquid lubrication technology can unite the advantages of solid and liquid lubricants to arise synergistic effect if it is properly used. For lamellar solid lubricants, the property of selective adsorption should be a significant factor to consider for their solid/liquid lubrication in future.

4. Conclusion

Two solid/liquid systems were successfully established by combining pure WS_2 films with FCPSO and SiCH, separately. The results revealed that the tribological performances of the composite systems were dominated by the selective adsorption of WS_2 crystallographic planes to special oils. The SiCH oil with more structure of hydrocarbon chains and weak polarity preferentially adsorbed with the basal plane of WS_2 films to form perfect lubricating and transfer films, resulting in a synergistic lubricating effect which brought about significant improvement in the tribological properties. However, the WS_2/FCPSO system did not generate the synergistic lubricating effect due to the polarity of FCPSO oil as well as the absent of hydrocarbon chains in the molecular structure. Over all**,** the property of selective adsorption should be a key factor to consider to the lamellar lubricant based solid/liquid lubrication system.

Acknowledgements

This work was supported by National Key Basic Research Program of China (973) (Grant No.2013CB632302) and National Science Foundation of China (Grant No. 51305427). The authors gratefully acknowledge Prof. Dapeng Feng at State Key Laboratory of Solid Lubrication, Lanzhou Institute of Chemical Physics for offering the lubricating oils.

References

1. M. J. Dube, D. Bollea, W. R. Jr. Jones, M. Marchetti, M. J. Jansen, A new synthetic hydrocarbon liquid lubricant for space applications, *Tribol. Lett*., 2003, **15,** 3-8.
2. J. R. Jones, M. J. Jansen, Space Tribology, *NASA/TM*-209924, 2000.
3. H. Song, L. Ji, H. X. Li, X. H. Liu, H. D. Zhou, W. Q. Wang, J. M. Cheng, Perspectives of friction mechanism of a-C:H film in vacuum concerning the onion-like carbon transformation at the sliding interface, *RSC Adv*., 2015, **5**, 8904-8911.
4. D. M. Hunten, R. P. Turco, O. B. Toon, Smoke and dust particles of meteoric origin in the mesosphere and stratosphere, *J. Atmos. Sci*., 1980, **37,** 1342-1357.
5. X. F. Liu, L. P. Wang, J. B. Pu, Q. J. Xue, Surface composition variation and high-vacuum performance of DLC/ILs solid–liquid lubricating coatings: Influence of space irradiation, *Appl. Surf. Sci*., 2012, **258,** 8289-8297.
6. X. F. Liu, L. P. Wang, Q. J. Xue, DLC-based solid–liquid synergetic lubricating coatings for improving tribological behavior of boundary lubricated surfaces under high vacuum condition, *Wear*, 2011, **271,** 889-898.
7. X. F. Liu, L. P. Wang, Q. J. Xue, High vacuum tribological performance of DLC-based

solid–liquid lubricating coatings: Influence of atomic oxygen and ultraviolet irradiation, *Tribol. Int*., 2013, **60,** 36-44.

8. X. F. Liu, L. P. Wang, Q. J. Xue, A novel carbon-based solid–liquid duplex lubricating coating with super-high tribological performance for space applications, *Surf. Coat. Technol*., 2011, **205,** 2738-2746.
9. A. Erdemir, R. Erck, G. Fenske, H. Hong, Solid/liquid lubrication of ceramics at elevated temperatures, *Wear*, 1997, **203,** 588-595.
10. A. Erdemir, O. Ajayi, G. Fenske, R. Erck, J. Hsieh, The synergistic effects of solid and liquid lubrication on the tribological behavior of transformation-toughened ZrO_2 ceramics, *Tribol. Trans*., 1992, **35,** 287-297.
11. X. F. Liu, L. P. Wang, Z. B. Lu, Q. J. Xue, Vacuum tribological performance of DLC-based solid–liquid lubricating coatings: Influence of sliding mating materials, *Wear*, 2012, **292,** 124-134.
12. M. Ratoi, V. B. Niste, J. Zekonyte, WS_2 nanoparticles-potential replacement for ZDDP and friction modifier additives, *RSC Adv*., 2014, **4**, 21238-21245.
13. J. Y. Hao, P. Wang, X. Q. Liu, W. M. Liu, Solid lubricating film/oil or grease complex system II:tribological properties of DLC film coated with space oils and the related greases, *Tribology*, 2010, **30,** 217-222. (*In Chinese*).
14. G. Y. Bai, J. Q. Wang, Z. G. Yang, H. G. Wang, Z. F. Wang, S. R. Yang, Preparation of a highly effective lubricating oil additive-ceria/graphene composite, *RSC Adv*., 2014, **4**, 47096-47105.
15. A. Erdemir, Review of engineered tribological interfaces for improved boundary lubrication, *Tribol. Int*., 2005, **38,** 249-256.
16. N. Renevier, J. Hamphire, V. Fox, J. Witts, T. Allen, D. Teer, Advantages of using self-lubricating, hard, wear-resistant MoS_2-based coatings, *Surf. Coat. Technol*., 2001, **142,** 67-77.
17. S. S. Xu, X. M. Gao, M. Hu, J. Y. Sun, D. S. Wang, F. Zhou, L. J. Weng, W. M. Liu, Morphology evolution of Ag alloyed WS_2 films and the significantly enhanced mechanical and tribological properties, *Surf. Coat. Technol*., 2014, **238,** 197-206.
18. S. S. Xu, X. M. Gao, M. Hu, J. Y. Sun, D. S. Wang, F. Zhou, L. J. Weng, W. M. Liu, Nanostructured WS_2–Ni composite films for improved oxidation, resistance and tribological performance, *Appl. Surf. Sci*., 2014, **288,** 15-25.
19. S. S. Xu, X. M. Gao, M. Hu, J. Y. Sun, D. S. Wang, F. Zhou, L. J. Weng, W. M. Liu, Microstructure evolution and enhanced tribological properties of Cu dopped WS_2 films, *Tribol. Lett*., 2014, **55,** 1-13.
20. Y. Y. Wu, H. X. Li, L. Ji, L. Lu, Y. P. Ye, J. M. Cheng, H. D. Zhou, Structure, mechanical and tribological properties of MoS_2/a-C:H composite films, *Tribol. Lett*., 2013, **52,** 371-380.
21. C. Donnet, J. Martin, M. T. Le, M. Belin, Super-low friction of MoS_2 coatings in various environments, *Tribol. Int*., 1996, **29,** 123-128.
22. T. Spalvins, Frictional and morphological properties of Au-MoS_2 films sputtered from a compact target, *Thin Solid Films*, 1984, **118,** 375-384.
23. Lancaster, J, Anisotropy in the mechanical properties of lamellar solids and its effect on wear and transfer, *Wear*, 1966, **9,** 169-188.
24. R. W. G. Wyckoff, *Crystal Structures*, Interscience Publishers, New York, 2nd ed., 1963.

25. S. S. Xu, X. M. Gao, M. Hu, J. Y. Sun, D. Jiang, D. S. Wang, F. Zhou, L. J. Weng, W. M. Liu, Dependence of atomic oxygen resistance and the tribological properties on microstructures of WS_2 films, *Appl. Surf.* Sci., 2014, **298,** 36-43.
26. A. J. Groszek, Preferential adsorption of long-chain normal paraffins on MoS_2, WS_2 and Graphite from n-Heptane, *Nature*, 1964, **204,** 680.
27. A. J. Groszek, R. Witheridge, Surface properties and lubricating action of graphite and MoS_2, *Tribol. Trans*., 1971, **14,** 254-266.
28. G. Andrews, A. J. Groszek, N. Hairs, Measurement of surface areas of basal plane and polar sites in graphite and MoS_2 powders, *Tribol. Trans*., 1972, **15,** 184-191.
29. A. J. Groszek, Selective adsorption at graphite/hydrocarbon interfaces, *P. Roy. Soc. A-Math. Phy*., 1970, **314,** 473-498.
30. H. E. Kern, G. H. Findenegg, Adsorption from solution of long-chain hydrocarbons onto graphite: surface excess and enthalpy of displacement isotherms, *J. Colloid. Interf. Sci*., 1980, **75,** 346-356.
31. A. J. Groszek, Oleophilic surface and anti-wear action of solid lubricants, *Proc. Inst*., 1967, **182,** 1967-68.
32. A. J. Groszek, Preferential adsorption of alcohols of iron/n-heptane interfaces, *Soc. Chem. Ind*., 1968, **28,** 174-187.
33. A. J. Groszek, Preferential adsorption of compounds with long methylene chains on cast iron, graphite, boron nitride, and molybdenum disulfide, *Tribol. Trans*., 1966, **9,** 67-76.
34. A. J. Groszek, Preferential adsorption of normal hydrocarbons on cast iron, *Nature*, 1962, **196,** 531-533.
35. L. J. Weng, H. Z. Wang, D. P. Feng, W. M. Liu, Q. J. Xue, Tribological behavior of the synthetic chlorine-and fluorine-containing silicon oil as aerospace lubricant, *Ind. Lubr. Tribol*., 2008, **60,** 216-22. (*In Chinese*).
36. H. Z. Wang, S. W. Zhang, D. Qiao, D. P. Feng, W. M. Liu, Tribological performance of silahydrocarbons used as steel-steel lubricants under vacuum and atmospheric pressure, *J. Nanomater*., 2014, **2014,** 1-8.
37. J. R. Jones, M. Jansen, L. Gschwender, J. R. Snyder, S. Sharma, R. Predmore, M. Dube, The tribological properties of several silahydrocarbons for use in space mechanisms, *Lubr. Sci*., 2004, **20,** 303-315.
38. I. J. Zabinsk, M. Donley, S. Walck, T. Schneider, N. McDevitt, The effects of dopants on the chemistry and tribology of sputter-deposited MoS_2 films, *Tribol. Trans*., 1995, **38,** 894-904.
39. T. Scharf, A. Rajendran, R. Banerjee, F. Sequeda, Growth, structure and friction behavior of titanium doped tungsten disulphide (Ti-WS_2) nanocomposite thin films, *Thin Solid Films*, 2009, **517,** 5666-5675.
40. M. Masuko, K. Kishi, A. Suzuki, S. Obara, The lifetime of boundary lubrication performance of small-quantity-applied liquid lubricants for space mechanisms evaluated with a vacuum reciprocating tribometer, *Tribol. Trans*., 2009, **53,** 75-83.
41. S. W. Zhang, L. T. Hu, H. Z. Wang, D. P. Feng, Tribological Behaviors of Two Kinds of Fluorine-containing Space Lubricating Oil in Vacuum, *Tribology*, 2012, **32,** 619-625. (*In Chinese*).
42. J. Giltrow, A. J. Groszek, The effect of particle shape on the abrasiveness of lamellar solids, *Wear*, 1969, **13**, 317-3.